Proc. of the 10th International OFDM Workshop
(InOWo 2005),
Hamburg, Germany, pp. 109-113, Aug. 2005.

Backwards compatibility for MIMO systems based on IEEE 802.11a

Tim C.W. Schenk* and Bas Driesen‡
*Eindhoven University of Technology, Radiocommunication Chair, PO Box 513, 5600 MB Eindhoven, The Netherlands,
Tel. +31 40 247 3436, Fax. +31 40 245 5197, T.C.W.Schenk@tue.nl
‡Philips Consumer Electronics, Innovation Lab, Glaslaan 2, Eindhoven, The Netherlands, Bas.Driesen@philips.com

***Abstract*— In this contribution we study different possibilities for backwards compatibility (BWC) on the physical layer for multiple-input multiple-output (MIMO) based wireless local-area networks (WLANs) with IEEE 802.11a based systems operating in the same band. The requirements for BWC are reviewed and based on these constraints different packet structures are proposed. The performances of these structures are compared in terms of mean-squared-error (MSE) in channel estimation, MSE in carrier frequency offset estimation and bit-error-rate. It is concluded that subcarrier orthogonal and subcarrier multiplexed preambles are promising for a low number of TX branches and low delay spreads, but that when these parameters are high, structures with a higher overhead ratio are required.**

I. Introduction

THE MAIN design goals of next generation WLANs are a significant increase in bit rate and network capacity compared to currently deployed systems. The application of multiple antennas at both transmitter (TX) as receiver (RX) side of wireless communication systems is proposed in many contributions over the last few years as a solution to reach these goals. The combination of these MIMO techniques with orthogonal frequency division multiplexing (OFDM) for broadband systems is seen as a promising basis for high data rate wireless systems [1]. This is especially the case for WLAN, which more and more are based on the IEEE standards 802.11a [2] and g [3], since they already use OFDM.

Since the spectrum is scarce, however, these new systems will have to operate in the same frequency band as the already deployed single-input single-output (SISO) systems. This forces the MIMO systems to exhibit some kind of backwards compatibility (BWC) with these existing systems, to enable efficient co-existence. Although BWC is possible on different layers in the OSI stack, it was shown by Boer et. al. in [4] that it is achieved most efficiently on the physical layer (PHY). That is why this contribution regards PHY BWC of a MIMO extension of the OFDM-based IEEE 802.11a standard.

The paper reviews the packet and preamble structure of IEEE 802.11a based systems and explains the requirements for BWC with these kind of systems. Different BWC packet structures are presented. Subsequently, the performances of systems based on the different preambles are compared. Hereto the mean-squared error (MSE) in channel estimation, the influence of timing offsets, the MSE in carrier frequency offset (CFO) estimation and bit-error-rate (BER) performance are regarded.

This work was sponsored by the Dutch cooperative research project B4 BroadBand Radio@Hand (BTS01063) and by Agere System Inc.

II. System Description

Consider a MIMO OFDM system with N_t TX and N_r RX branches, denoted here as a $N_t \times N_r$ system, which applies MIMO processing at the receiver.

Let us define the MIMO OFDM vector to be transmitted during a symbol period as $\mathbf{s} = \left[\mathbf{s}_1^T, \mathbf{s}_2^T, \ldots, \mathbf{s}_{N_t}^T\right]^T$, where $\mathbf{s}_{n_t}$ denotes the $N_c \times 1$ frequency domain transmit vector for the n_tth TX and N_c represents the number of subcarriers. This vector is transformed to the time domain using the inverse discrete Fourier transform (IDFT) and a cyclic prefix (CP) is added. The signal is then transmitted through the quasi-static multipath channel $\mathbf{C}$.

At the RX the signals are impaired by additive zero-mean complex white Gaussian noise (AWGN), denoted by $\mathbf{v}$. The system is synchronized in frequency and time domain. Subsequently, an estimate of the channel matrix $\mathbf{C}$ is acquired. Thereafter, the CP is removed and the received signal is converted to the frequency domain using the DFT. With perfect synchronization this yields the $N_c N_r \times 1$ RX vector

$$\mathbf{x} = \mathbf{H}\mathbf{s} + \mathbf{n} \ , \tag{1}$$

where $\mathbf{H}$ is the $N_c N_r \times N_c N_t$ channel matrix, i.e., the frequency domain equivalent of $\mathbf{C}$. The (n_r, n_t)th block element of $\mathbf{H}$ is $\mathbf{H}_{n_r n_t}$, the $N_c \times N_c$ diagonal channel matrix between the n_tth TX and n_rth RX. $\mathbf{n}$ represents the frequency-domain equivalent of $\mathbf{v}$. Since the channel consists of diagonal channel blocks, the MIMO processing can be applied per subcarrier, yielding the $N_c N_t \times 1$ estimate of the transmitted symbol vector $\mathbf{s}$.

III. Packet Structure for MIMO WLAN

This section reviews the IEEE 802.11a PHY frame format and regards the requirements for BWC with this packet structure. Subsequently, four possible BWC MIMO packet structures are proposed.

A. IEEE 802.11a Frame Format

The structure of an 802.11a frame is depicted schematically in Fig. 1. The structure consists of 4 parts, where the first 3 parts form the *Preamble* and the last part (DATA) is the actual data transmitted in the packet.

Fig. 1. PHY frame format IEEE 802.11a.

The first part of the preamble consists of a ten times repeated short training symbol of 16 samples, as a whole denoted by ST. This part is in the RX used to detect

the packet, adjust the automatic-gain-control settings and derive a coarse estimate of the CFO. The second part is a twice repeated long training symbol of 64 samples, with an extended cyclic prefix of 32 samples, altogether denoted by LT. This part is used for channel estimation, fine CFO estimation and symbol timing. The last part of the preamble is formed by the SIGNAL field, which contains information about the transmission, including the packet length, modulation size and coding rate.

In the remainder we will not regard the ST part of the preamble, since the LT and SIGNAL field were identified as the most crucial parts in creating a BWC MIMO frame format. The (frequency domain) $N_c N_r \times 2$ received signal during the LT-part of the preamble can be written as

$$\mathbf{X}_{\mathrm{p}} = \mathbf{H}\mathbf{S}_{\mathrm{p}} + \mathbf{N} \ , \tag{2}$$

where the subscript p refers to the preamble period. Furthermore, the transmitted frequency domain LT-block, as defined in [2], is given by $\mathbf{S}_{\mathrm{p}} = [1, 1] \otimes \mathbf{s}_{\mathrm{p}}$, where $\otimes$ denotes the Kronecker product. The matrices $\mathbf{X}_{\mathrm{p}}$ and $\mathbf{N}$ exhibit the same structure as $\mathbf{S}_{\mathrm{p}}$.

From $\mathbf{X}_{\mathrm{p}}$ we can draw the least-squares (LS) estimate of the channel matrix, which is found by multiplication with the pseudo-inverse of the LT block $\mathbf{S}_{\mathrm{p}}$:

$$\tilde{\mathbf{H}} \quad = \mathbf{X}_{\mathrm{p}}\mathbf{S}_{\mathrm{p}}^{\dagger} = \mathbf{H} + \mathbf{N}\mathbf{S}_{\mathrm{p}}^{\dagger} \ . \tag{3}$$

B. BWC Requirements

The multiple-access scheme of IEEE 802.11a depends on the fact that a station (STA) does not access the wireless medium while another STA, or access point (AP), is transmitting. When a STA detects in the DATA part of the packet that the packet is intended for another STA or when the STA can not decode the packet, it will not transmit data for the time corresponding to the packet length it has detected from the SIGNAL field.

It is, therefore, crucial that in a mixed-mode environment, where SISO as well as MIMO transmissions occur, the SISO terminals can decode the packet upto the end of the SIGNAL field. In this way the SISO STA can detect the packet duration and defer for this time period and not interfere the MIMO transmission. For the MIMO terminal there is no problem in detecting and decoding the SISO transmission.

The main requirement for BWC is thus that the SISO terminal can detect the SIGNAL field of the MIMO transmission, which has to be equal to the SISO SIGNAL field, so it knows the length of the MIMO transmission.

C. MIMO PHY Frame Format

Next to the BWC requirements, the preamble part of the MIMO transmission has to facilitate channel estimation and synchronization. Figure 2 presents four PHY frame formats which conform to these prerequisites. The figure shows the frame structures for a system applying two spatial streams. It is noted that the SIGNAL field depicted here can be followed by an extra MIMO SIGNAL field, which holds extra information about the MIMO transmission, but this is not considered in this paper.

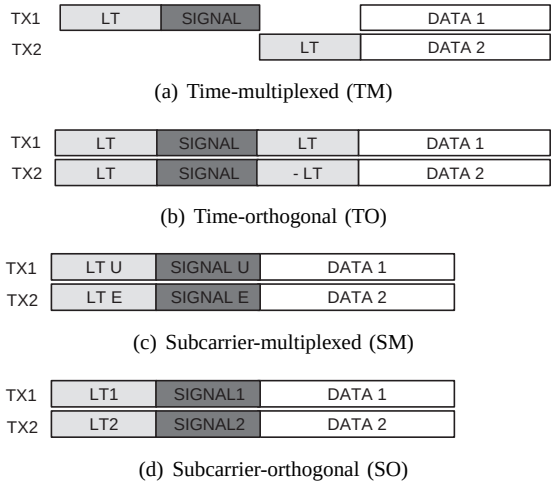

(a) Time-multiplexed (TM)

(b) Time-orthogonal (TO)

(c) Subcarrier-multiplexed (SM)

(d) Subcarrier-orthogonal (SO)

Fig. 2. Backwards compatible MIMO PHY frame formats.

1) Time-Multiplexed: The first structure is the time-multiplexed (TM) preamble as depicted in Fig. 2(a). Here the LT symbols are sequentially send from the different TXs. The TX that transmits the first LT, also transmits the SIGNAL field. A SISO RX observes a SISO transmission and can thus detect the SIGNAL field. If we write the LT-part of the preamble as function of the SISO LT symbols $\mathbf{S}_{\mathrm{p}}$, we get

$$\mathbf{S}_{\mathrm{p,TM}} = \mathbf{I}_{N_t} \otimes \mathbf{S}_{\mathrm{p}} \ . \tag{4}$$

For this structure $(N_t - 1)$ LT blocks have to be transmitted after the SIGNAL field.

A clear disadvantage of this concept is that during the preamble phase the total TX power is N_t times smaller then during the other parts of the transmission. This can be overcome by increasing the TX power of the TX branches during the preamble phase. This is, however, not considered in this paper.

2) Time-Orthogonal: Figure 2(b) depicts the time-orthogonal (TO) preamble. Upto the end of the SIGNAL field the frame format on all TX branches is equal. This means that the SISO RX effectively sees and estimates a channel which is the sum of the channel elements corresponding to the different TX branches. Orthogonality is achieved by using a Walsh-Hadamard or Fourier matrix, which are given by $[1, 1; 1, -1]$ for the 2 TX case. We can rewrite the LT-part of the preamble as

$$\mathbf{S}_{\mathrm{p,TO}} = \mathbf{\Phi}_{N_t} \otimes \mathbf{S}_{\mathrm{p}} \ , \tag{5}$$

where $\mathbf{\Phi}_{N_t}$ denotes the orthogonal matrix. When $\mathbf{\Phi}_{N_t}$ equals the Walsh-Hadamard matrix or the Fourier matrix, $(2^{\lceil \log_2(N_t) \rceil} - 1)$ or $(N_t - 1)$ LT blocks after the SIGNAL field are required, respectively.

3) Subcarrier-Multiplexed: The subcarrier-multiplexed (SM) preamble is depicted in Fig. 2(c). Here the preamble is transmitted simultaneously on all TXs, not increasing the overhead compared to a SISO system. TXn_t transmits the original training symbol on subcarriers $\{n_t, N_t + n_t, \ldots, N_c - N_t + n_t\}$, where we assumed N_c to be a multiple of N_t. For the example in Fig. 2(c) this means TX1 and TX2 transmit on the uneven (U) and even (E) subcarriers, respectively. The corresponding carriers of the

SIGNAL field are transmitted on the same TX. The SISO RX sees and estimates the combined (interleaved) channel and can detect the SIGNAL field.

The LT-part of the preamble can now be written as

$$\mathbf{S}_{\text{p,SM}} = [1,1] \otimes [(\mathbf{s}_\text{p} \circ \boldsymbol{\theta}_1)^T, (\mathbf{s}_\text{p} \circ \boldsymbol{\theta}_2)^T, \ldots, (\mathbf{s}_\text{p} \circ \boldsymbol{\theta}_{N_t})^T]^T, \quad (6)$$

where $\circ$ denotes element-wise multiplication and the $N_c \times 1$ subcarrier interleaving vector for TXn_t is given by

$$\boldsymbol{\theta}_{n_t} = \mathcal{C}_{n_t-1}\{[1, \mathbf{0}_{N_t-1}, 1, \mathbf{0}_{N_t-1}, \ldots, 1, \mathbf{0}_{N_t-1}]\}^T. \quad (7)$$

Here $\mathbf{0}_M$ denotes the $1 \times M$ all zero vector and the function $\mathcal{C}_m\{\cdot\}$ cyclicly shifts its argument over m samples.

4) Subcarrier-Orthogonal: The subcarrier-orthogonal (SO) preamble, as depicted in Fig. 2(d), also achieves orthogonality in the frequency domain. The long training symbols are multiplied with orthogonal vectors. When the SIGNAL field is multiplied with the same vectors, the SISO RX is able to detect the SIGNAL field. It is noted that this concept also does not increase the overhead compared to a SISO transmission.

When Fourier sequences are applied as orthogonal sequences, the transmitted LT-part of the preamble is given by

$$\mathbf{S}_{\text{p,SO}} = [1,1] \otimes [(\mathbf{s}_\text{p} \circ \boldsymbol{\zeta}_1)^T, (\mathbf{s}_\text{p} \circ \boldsymbol{\zeta}_2)^T, \ldots, (\mathbf{s}_\text{p} \circ \boldsymbol{\zeta}_{N_t})^T]^T, \quad (8)$$

where $\boldsymbol{\zeta}_{n_t}$ equals the $(1+(n_t-1)\lfloor N_c/N_t \rfloor)$th column of the Fourier matrix. It is noted that this preamble structure corresponds to what is sometimes referred to as *cyclic delay* preamble.

IV. Performance Evaluation

In this section we regard the performance of systems using the four preambles proposed in Section III-C. In all simulations uncorrelated Rayleigh faded channels with an exponential decaying power-delay-profile were applied. All system parameters were based on the IEEE 802.11a standard [2].

A. Channel Estimation

The channel estimate for the TM and TO preamble can be found by using the LS approach as described in (3), by replacing $\mathbf{S}_\text{p}$ by the MIMO LT-parts $\mathbf{S}_{\text{p,TM}}$ and $\mathbf{S}_{\text{p,TO}}$, respectively. For the SM and SO preamble, however, this does not provide estimates on all carriers, requiring interpolation and extrapolation to find the channel response on the remaining carriers. In this paper we will consider linear and cubic interpolation [5].

It is noted that per subcarrier LS estimation, i.e., without interpolation, is also possible for the SO and SM based preamble. Then spatial shifted versions of $\mathbf{S}_{\text{p,SO}}$ and $\mathbf{S}_{\text{p,SM}}$ have to be transmitted after the SIGNAL field. The overhead ratio increases to that of the TO and TM preamble.

Figure 3 shows the MSE as function of the subcarrier index for the estimation of the channel elements $\mathbf{H}_{11}$ for a 2×2 system. The rms delay spread was 50 ns and cubic interpolation was used for the SO and SM based method.

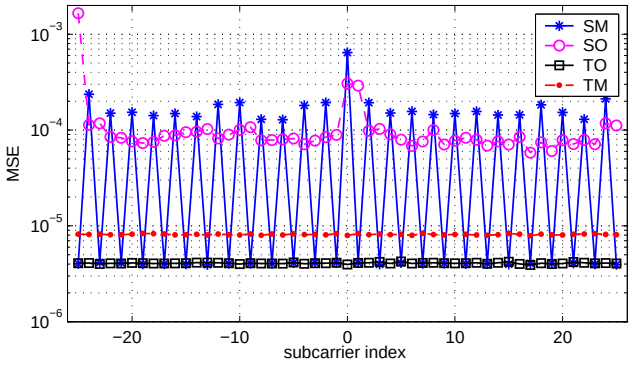

Fig. 3. MSE in channel estimation as function of the subcarrier index for a 2×2 system. Rms delay spread = 50 ns and SNR = 50 dB.

It is observed that for the estimates based on the TM and TO preamble, the MSE is flat over the carriers, since a pilot is transmitted on all carriers. The level of the MSE is determined by the SNR. For the SO and SM based estimation, however, also inter- and extrapolation errors occur. It can be concluded from Fig. 3 that for the SM based estimation half of the carriers is limited in performance by the AWGN, and the other half is limited in performance by the interpolation errors. For the SO based estimation, the course of the MSE curve is more flat, since the estimates on all carriers are influenced by the interpolation. For both SO and SM higher errors occur near DC and the edges of the spectrum due to extrapolation, which is inherently less accurate then interpolation.

The MSE (averaged over all carriers) is depicted in Fig. 4 as function of the SNR for rms delay spreads of 50 and 100 ns.

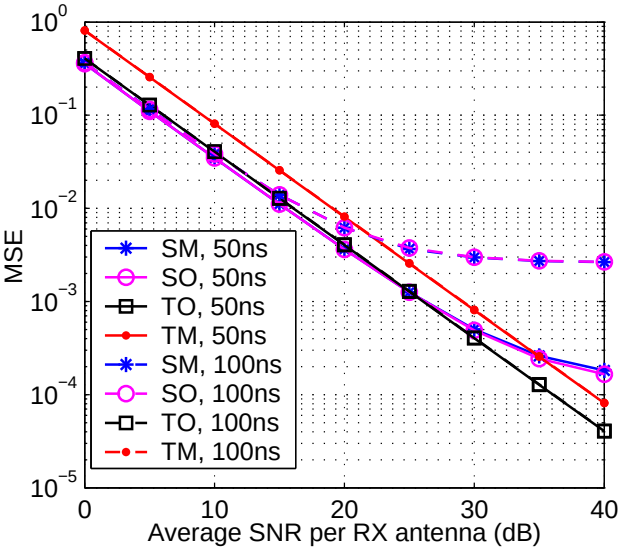

Fig. 4. Comparison of the MSE in channel estimation as function of the SNR. Results are given for a 2×2 system applying different preambles and for rms delay spreads of 50 ns (—) and 100 ns (– –).

It can be concluded from this figure that the TO method always performs better than the TM method, since more signal energy is received. Both curves show no flooring

and do not dependent on the rms delay spread. For low SNRs the SO and SM method perform best, since the cubic interpolation results in noise-averaging here. For high SNRs flooring occurs in the MSE curves, due to inter- and extrapolation errors. These errors increase when the delay spread increases.

The flooring of the MSE is further investigated in Fig. 5, where the level of the MSE floor at high SNR is depicted as function of the rms delay spread for a 2×2 and 4×4 system, where we applied both linear and cubic interpolation.

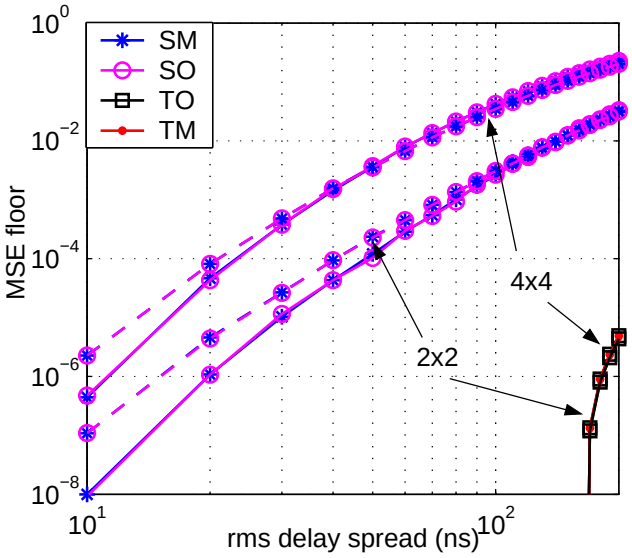

Fig. 5. MSE floor in channel estimation for a 2×2 and 4×4 system as function of the rms delay spread. Results are given for cubic (—) and linear (−−) interpolation.

Clearly the MSE floor increases with increasing rms delay spread for both the SM and SO based channel estimation, which show similar performance. At high delay spreads, however, also flooring occurs for the TM and TO based estimation, which is explained by inter-symbol-interference (ISI) between the preamble symbols. The flooring for the TM and TO preamble, therefore, does not depend on the MIMO configuration. The MSE floor for SM and SO, however, increases with increasing number of TX branches. This is explained by the fact that more interpolation is necessary, since less observations per TX branch are available. When we compare the performance of the two interpolation techniques, it can be concluded that at low delay spreads the cubic interpolation performs best, but that the linear interpolation performs better at high values of delay spread. This is explained by the fact that correlation between neighboring carriers decreases with increasing rms delay spread. Since this cubic interpolation takes into account multiple neighboring carriers, this results in errors at high delay spreads.

Applying interpolation to estimate channel response is sensitive to timing offsets from the ideal timing point [6]. These offset introduce phase rotations in the frequency domain, which increase with increasing offset. When these phase rotations are too high, they can result in interpolation errors. The influence of these offsets on the MSE floor of the SM based channel estimation is given in Fig. 6 for a 2×2 and 4×4 system for rms delay spreads of 50 and 100 ns.

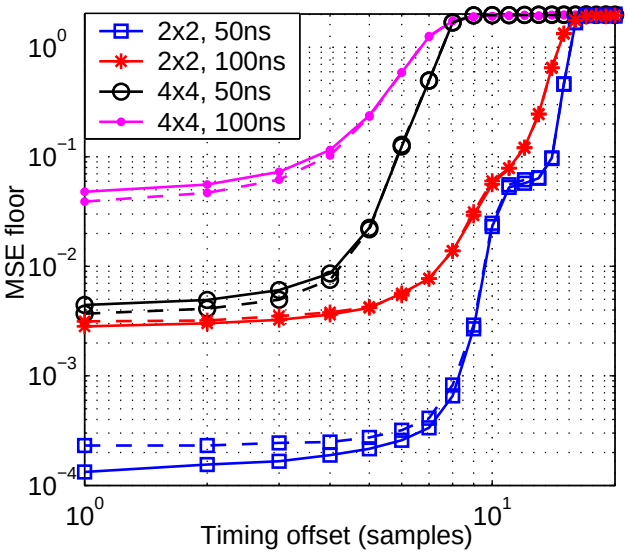

Fig. 6. MSE floor in channel estimation for the SM preamble for a 2×2 and 4×4 system as function of the timing offsets for a rms delay spread of 50 ns and 100 ns. Results are given for cubic (—) and linear (−−) interpolation.

It can be concluded from this figure that the MSE floor increases when the timing offset increases. When the delay spread or number of TX branches increases, the sensitivity to timing offset increases. Furthermore, it is concluded that for these rms delay spreads the 2 TX case the cubic interpolation outperforms linear interpolation at low timing offsets, but that for the 4 TX case the linear interpolation outperforms the cubic.

B. *Frequency Synchronization*

Since all preamble structures of Section III-C have repeated symbols, we can apply frequency synchronization in the time-domain applying the method proposed for SISO systems by [7]. This method correlates the two symbols and the phase of this correlation then linearly relates to the CFO. Similar to the MIMO evaluation in [8] we assume that all TXs and all RXs have a common oscillator and that, thus, a single CFO between the TX and RX exists.

In [8] we found that the Cramer-Rao lower bound (CRLB) on estimation of the (subcarrier spacing normalized) CFO ε in an AWGN channel was given by

$$\mathrm{var}(\varepsilon) \geq ((2\pi)^2 N_r N_c N_p \rho)^{-1} \quad , \tag{9}$$

where ρ denotes the SNR during the preamble phase and N_p denotes the number of LT-blocks.

We regard the MSE in estimation of ε by a SISO system, which has to detect the SIGNAL field, and by a MIMO system, which also has to decode the data part of the frame. For the SISO system we, therefore, regard the LT-part upto the SIGNAL field and for the MIMO system the whole LT-part.

Fig. 7 presents MSE results from Monte-Carlo simulations for a SISO and 4×4 system for a rms delay spread of 10 ns. The CRLB for CFO estimation based on the SO and SM preamble ($N_p = 1$) is plotted as reference.

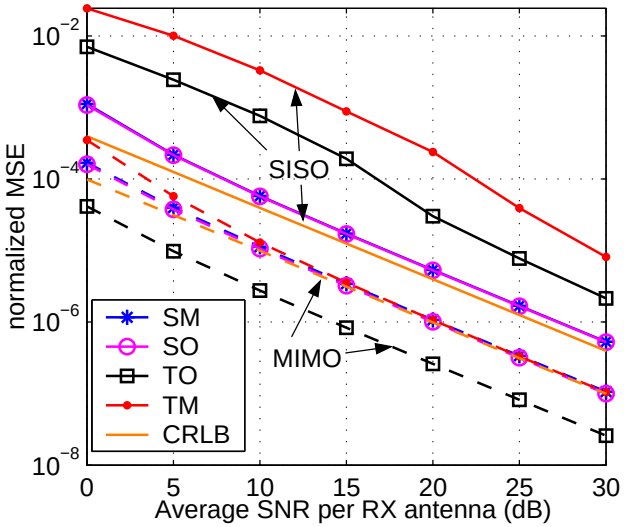

Fig. 7. MSE in CFO estimation (normalized to the subcarrier spacing) for different preamble formats as function of the SNR for a SISO (—) and 4×4 (−−) system and a rms delay spread of 10 ns.

It can be concluded from Fig. 7 that for the SISO system the SO and SM approach the CRLB, which is explained by frequency diversity introduced by the preamble structure. The TO and TM preamble do not exploit this diversity and, therefore, perform considerably worse. The TM approach performs 6 dB worse than the TO method, since 6 dB less energy is received.

For the MIMO case the SO, SM and TM method achieve the plotted CRLB, since now also the space diversity is exploited. The TO method performs 6 dB better, since 6 dB more power is received than in the other three cases. When the delay spread is increased further the MIMO curves do not change, the SISO curves, however, come closer to the SISO CRLB.

C. BER Performance

The BER performance of a 2×2 MIMO 802.11a extension is given in Fig. 8 for data rates of 12 Mbps (BPSK, rate 1/2) and 108 Mbps (64-QAM, rate 3/4). The RX applies channel estimation using the proposed preambles. Frequency synchronization is assumed perfect. Zero-Forcing is used as MIMO estimation algorithm, which feeds soft-values to the Viterbi decoder. Results are given for a rms delay spread of 50 ns. Cubic interpolation is used in channel estimation.

The results in Fig. 8 show that for 12 Mbps, the systems based on the SM, SO and TO preamble perform 1.5 dB worse, at a BER of 10^{-4}, than the ideal case with perfect channel knowledge. The TM performs another 1.5 dB worse. For the 108 Mbps we see the same differences at low SNRs, however, the SM and SO based methods show flooring in the BER curve, which can be explained by flooring in the MSE curve of the channel estimation.

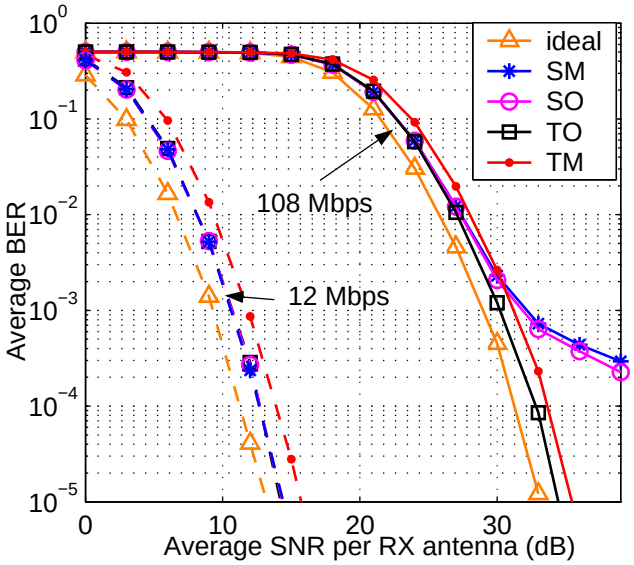

Fig. 8. BER performance of a 2×2 system applying the different preamble formats. Results are given for BPSK, rate 1/2 coding (12 Mbps) and 64-QAM, rate 3/4 coding (108 Mbps).

V. Conclusions and Discussion

To create efficient backwards compatibility (BWC) of next-generation MIMO systems with currently deployed IEEE 802.11a/g systems, four BWC MIMO frame format concepts are presented. The performances of these concepts in terms of MSE in channel estimation, MSE in CFO estimation and BER are tested.

It is concluded that for low delay spreads, low number of TX branches and low timing offsets the SO and SM method are very well applicable, since they introduce no extra overhead compared to the SISO preamble. When high delay spreads and high number of TX antennas should be supported, however, the TO and TM preamble are preferred, although they introduce a considerable overhead. More efficient structures can in this case also be achieved by combining the preamble concepts, for instance SM with TO. A further decrease in overhead can be achieved by not implementing the LT-part after the SIGNAL field as repeated symbols, but as separate symbols. This will, nevertheless, decrease the estimation performance.

References

[1] G.G. Raleigh and V.K. Jones, "Multivariate modulation and coding for wireless communication," *IEEE Journ. on Selected Areas in Commun.*, vol. 17, no. 5, pp. 851–866, May 1999.

[2] *IEEE 802.11a standard*, ISO/IEC 802-11:1999/Amd 1:2000(E).

[3] *IEEE 802.11g standard*, Further Higher-Speed Physical Layer Extension in the 2.4 GHz Band.

[4] J. Boer, B. Driesen, and P-P.S. Giesberts, "Backwards compatibility," in *IEEE 802.11-03/714r0*, Sept. 2003.

[5] E. Meijering, "A chronology of interpolation: From ancient astronomy to modern signal and image processing," *Proc. of the IEEE*, vol. 90, 2002.

[6] M-H. Hsieh and C-H. Wei, "Channel estimation for OFDM systems based on comb-type pilot arrangement in frequency selective fading channels," *IEEE Trans. on Consumer Electronics*, vol. 44, 1998.

[7] P.H. Moose, "A technique for orthogonal frequency division multiplexing frequency offset correction," *IEEE Trans. on Communications*, vol. 42, no. 10, pp. 2908–2914, Oct. 1994.

[8] T.C.W. Schenk and A. van Zelst, "Frequency synchronization for MIMO OFDM wireless LAN systems," in *Proc. VTC-Fall 2003*, Oct. 2003, vol. 2, pp. 781–785.